Journal of Atmospheric and Terrestrial Physics, Vol. 46, No. 6/7, pp. 489–499, 1984.
Printed in Great Britain.

0021-9169/84 $3.00 + .00
Pergamon Press Ltd.

EISCAT observations of plasma convection and the high-latitude, winter *F*-region during substorm activity

M. Lockwood,* A. D. Farmer,* H. J. Opgenoorth† and S. R. Crothers*

*Rutherford Appleton Laboratory, Chilton, Didcot, Oxon, OX11 0QX, U.K., and
†Kiruna Geophysical Institute, Uppsala Ionospheric Observatory,
S-75590 Uppsala, Sweden

(*Received for publication* 21 *February* 1984)

Abstract—A 24 h period of observations by the EISCAT radar and other ground-based instrumentation is used to study the role of plasma convection in determining the morphology of the high-latitude *F*-region during winter. It is suggested that, in the afternoon sector of the polar convection pattern, rapid zonal (westward) flows caused low *F*-region electron densities due to an extension of the mid-latitude trough far into the sunlit hemisphere. Low densities on the dawn side prior to 0600 UT may also have been due to a trough-like feature. Although the generation mechanism is unclear, the trough may be the fossil remnant of a substorm. Around midnight, high *F*-region densities were seen, probably due to plasma flow emerging from the cap through soft particle precipitation in the auroral oval. Two substorms occurred at times when the radar was south of the auroral oval. Both caused enhanced convection speeds, a swing to equatorward flow, enhanced *E*-region densities and a depleted *F*-region. The first was seen as a Westward Travelling Surge, and the swing to purely southward flow which followed the surge front did not return to westward flows until 80–110 min later. The Harang discontinuity was observed co-rotating eastwards between the substorms, 65 ± 30 min before the separatrix between the dawn and dusk convection cells.

1. INTRODUCTION

Large-scale convection of plasma is known to exert a controlling influence on the winter *F*-layer at high latitudes. Knudsen (1974) showed that rapid flows across the polar cap (of the order of 1 km s^{-1}) can explain the maintenance of high ionisation densities on the night-side. Conversely, if the velocity is low, plasma can spend long periods in regions where there is neither photo-ionisation nor particle precipitation, resulting in depletions, such as the mid-latitude trough (Spiro *et al.*, 1978) and the polar hole (Brinton *et al.*, 1978). A number of processes affect the plasma in the *F*-layer and topside ionosphere: heating and photo-ionisation by both directly incident and scattered solar photons; soft-particle precipitation; vertical component of motion due to thermospheric winds and electric fields; diffusion; polar-wind escape; energy-dependent chemical reaction rates; neutral composition effects. However, where a combination of these processes acts, the plasma density changes depend upon the speed with which the flux tubes move and the processes in the regions from which they have recently convected. This dependence on field-perpendicular motions is particularly important during winter, when solar photon input is restricted to a region around noon at lower latitudes.

The convection of high-latitude plasma is driven by a potential difference imposed across the polar cap by the interaction of the solar wind with the magnetosphere, and hence varying with the velocity of solar wind flow and with the orientation of the Interplanetary Magnetic Field (IMF) (Reiff *et al.*, 1981). Numerical simulation of the high-latitude *F*-region (Sojka *et al.*, 1981a,b) shows that the mid-latitude trough is deeper and has a greater extent in local time when the convection is weak and that the polar hole is absent when convection is strong. The cross-cap potential difference Φ is correlated with the interplanetary ε index and with *Kp* (Reiff *et al.*, 1981; Oliver *et al.*, 1983). Sojka and Schunk (1983) assumed such a relationship with *Kp* to model the *F*-region effects of variations in the cross-cap potential difference and auroral precipitation during a geomagnetic storm. The response time of the ionosphere to these storm-time changes is of the order of minutes in the lower *F*-region, where production and loss of plasma dominate. It rises with altitude to several hours in the topside, where the long time constants for diffusion from the source regions beneath delay the enhancement. During this time the plasma can convect over considerable distances and, hence, density enhancements are not confined to an auroral torus, as they are at lower heights. Such topside enhancements outside the oval have been observed following a substorm (Whitteker *et al.*, 1978).

The dependence of high-latitude convection on the IMF orientation is discussed and extensively referenced in Farmer *et al.* (1984). The most common situation is a southward IMF ($B_z < 0$), giving a simple two-celled convection pattern, although the exact details may vary considerably, as discussed in Heelis and HANSON (1980). They also found that the two-celled pattern could break up during prolonged periods of low magnetic activity, particularly on the night-side. OLIVER *et al.* (1983) found the dawn cell to be less clearly defined and more irregular when Kp is low. The occurrence of substorms generally increases convection speeds and expands the pattern to lower latitudes, without changing its two-celled form (HEPPNER, 1972; FOSTER *et al.*, 1981a,b), except for short-lived phenomena, as discussed in Section 4.ii.

The role of convective motions in the formation of the trough (SPIRO *et al.*, 1978; QUEGAN *et al.*, 1982) means that its location is dependent on the level of geomagnetic activity. The expanded convection pattern at high Kp moves the trough to lower latitudes, while the extent of the trough in local time is largely determined by the season, as the trough tends to be 'filled-in' by photo-ionisation. In summer it is restricted to a few hours around local midnight, whereas in winter it will encircle most of the polar cap (SPIRO, 1978; MOFFETT and QUEGAN, 1983). There have been several recent reports of observations of the extension of the trough into the sunlit hemisphere, particularly in winter (e.g. HOLT *et al.*, 1983; SOJKA *et al.*, 1983; EVANS *et al.*, 1983). At all times of the year the trough is at its lowest latitudes near midnight. In summer it is equatorward of Tromsø ($\Lambda = 66°$) for all but the quietest geomagnetic conditions. In winter the trough is expected at the Tromsø latitude for periods around both dawn and dusk (see, for example, the statistical model of HALCROW and NISBET, 1977).

On 25 November 1982, substorm activity occurred during a 24 h period when the EISCAT radar was operated in the EISCAT Common Programme Zero (CP0) mode. These observations give the field-aligned distribution of plasma and the field-perpendicular convective motions, so one can study the role of convection in determining the plasma density profile, and the changes to both this and the convection, during substorms.

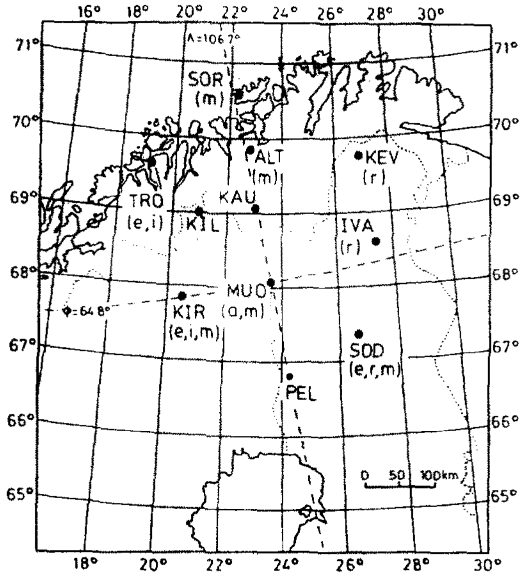

Fig. 1. Location of EISCAT receivers (e), riometers (r), magnetometers (m), ionosondes (i) and the all-sky camera (a) used in the study. The EISCAT receivers are at Tromsø (TRO), Sodankylä (SOD) and Kiruna (KIR). The all-sky camera is at Muonio (MUO), which is also near the centre of the magnetometer cross at corrected geomagnetic coordinates $\phi = 64.8°$, $\Lambda = 106.7°$. Other magnetometer stations are Sørøya (SOR), Alta (ALT), Kiruna, Sodankylä, Kautokeino (KAU), Kilpisjärvi (KIL), Kevo (KEV) and Pello (PEL). The last four of these were not operating on 25–26 November 1982. Riometers measuring absorption at 27.6 MHz are at Kevo, Ivalo (IVA) and Sodankylä.

2. OBSERVATIONS AND INSTRUMENTATION

The main data source for this investigation was the EISCAT radar [see Fig. 1 for the location and FARMER *et al.* (1984) for a description of the CP0 mode of operation and the analysis and data cleaning procedures]. There are some data gaps, especially in the vector velocities, since they require all three ground stations to be in operation, but most of the period from 1000 UT on 25 November to 1000 UT on 26 November provides electron density, N_e, electron temperature, T_e, ion temperature, T_i, and ion velocity height profiles. The raw data, recorded at 10 s time resolution, have been post-integrated into 5 min intervals and cleaned by excluding high variance and low signal-to-background noise (SNR) points. When velocities from all three sites were available, mutually orthogonal vector velocity components were calculated in a geomagnetic reference frame. The perpendicular components are plotted in Fig. 4.

Supporting data on E-region currents were obtained using the magnetometer cross shown in Fig. 1. Use was made, too, of the All-Sky Camera (ASC) at Muonio (HYPPÖNEN *et al.*, 1974), shown in the figure. The camera was running at the rate of 1 frame min^{-1}. Peak absorption values during each hour from the Sodankylä Geophysical Observatory's riometer chain provided an indication of the level of local auroral activity.

The interplanetary medium was monitored by the ISEE-3 spacecraft, which recorded the solar wind velocity and the IMF components. At this time it was at a position in Geocentric Solar Ecliptic coordinates (GSE) of $X = -92\ R_E$, $Y = -163\ R_E$ and $Z = 2\ R_E$. It was well outside the magnetosphere and bow shock, but, as Fig. 2b shows, there was poor geometry for comparisons to the environment at the Earth. We can probably expect some of the general features to be similar, albeit with a 20 min or so lag from Earth to spacecraft, but the ISEE-3 values should only be used with caution.

3. INTERPLANETARY AND GEOMAGNETIC CONDITIONS

Figure 2 summarises the ISEE-3 observations of B_z, the northward component of the IMF in the Geocentric Solar Magnetospheric (GSM) reference frame (Russell, 1971). B_z varied between -6.5 and $+4.4$ nT. On the whole, the IMF is weakly southward. However, there are periods, particularly 1100 to 1400 UT on the 25th and 1930 UT 25 November to 0130 UT 26 November, when it was persistently northward and spent long periods above the 1 nT level (dashed line in Fig. 2). Insofar as the ISEE IMF data is applicable to the Earth, the expectation is of mainly two-celled convection, with some periods (especially the 2 h each side of midnight) when this may give way to a more unstable pattern.

The 24 h period of EISCAT CP0 observations formed part of the recovery phase of a major (Kp 7+) geomagnetic storm which had its Sudden Commencement at 1100 UT on 24 November. By 1000 UT on 25 November, Kp had only fallen to 6−. The fall then continued down to 3o at 0300 UT on 26 November, when there was enhanced magnetic activity. The local magnetometer and riometer data is summarised in Fig. 3. There was a major substorm onset at 1710 UT, accompanied by a westward travelling surge. This can be seen in the detailed magnetograms in Fig. 5. A period of large and varying disturbances lasted until about 1820 UT. A second substorm was observed between 2150 UT and 2300 UT. These substorms were also seen as enhanced riometer absorption on the three Finnish riometers at Sodankylä, Ivalo and Kevo. The top panel of Fig. 3 shows the height at which the Tromsø beam falls into the Earth's shadow, the two dashed lines showing the height bounds of the observations. The lowest range gate, starting at an altitude of 128 km, is only in direct sunlight before 1500 UT on the 25th and after 0600 UT on the 26th. Key times from this graph are also shown as a guide on Figs. 6 and 7.

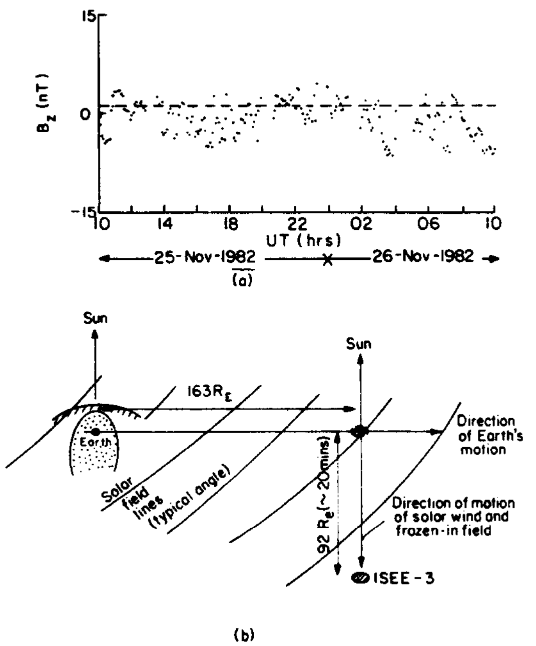

Fig. 2. (a) Top: northward component of the IMF (B_z) in Geocentric Magnetospheric coordinates observed by ISEE-3 during the period of CP0 observations on 25–26 November 1982. (b) Bottom: position of ISEE-3 with respect to the Earth and solar wind.

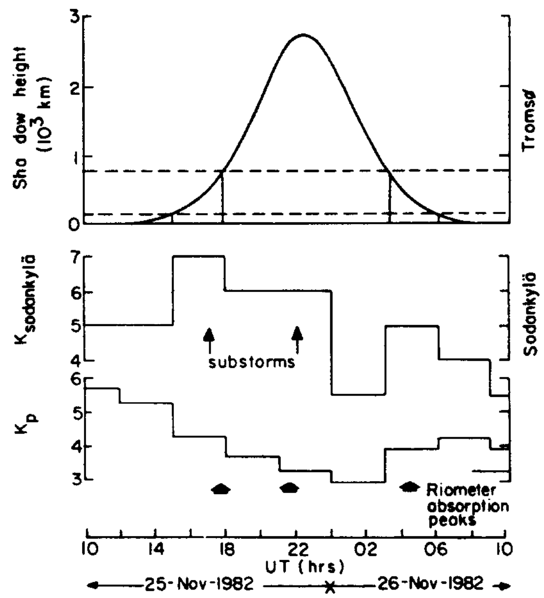

Fig. 3. The height of the Earth's shadow along the Tromsø beam, the local K index at Sodankylä, the planetary Kp index and the hourly peaks of riometer absorption observed at Kevo, Ivalo and Sodankylä during the period of CP0 observations on 25–26 November 1982.

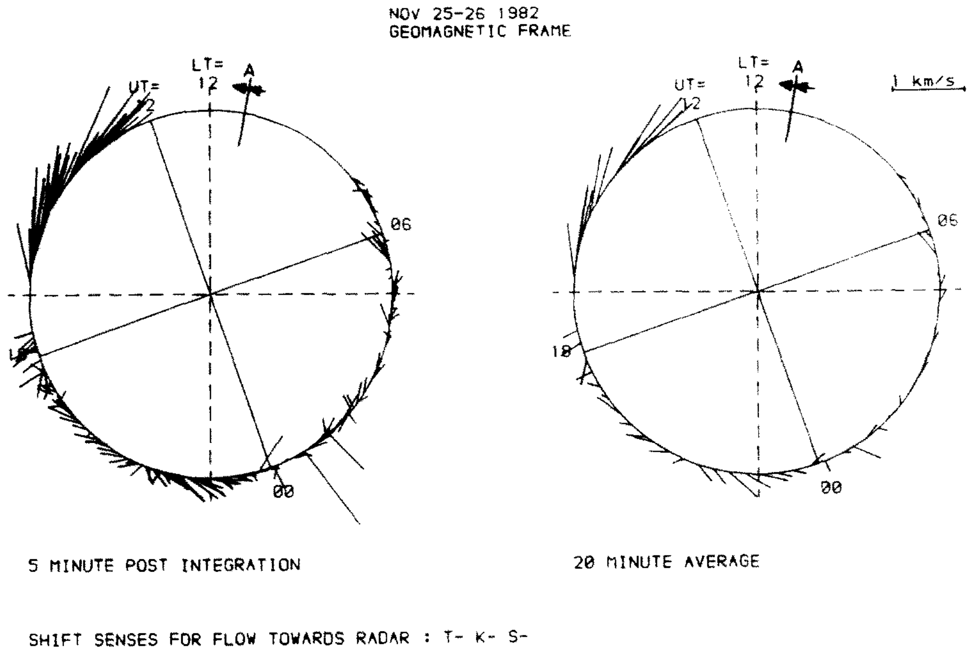

Fig. 4. Polar plot of field-perpendicular velocities. Each vector is plotted pointing away from the circular locus of the intersection scattering volume. A scale for the vectors is given in the top right and A denotes the start and end time of the 24 h observation run.

4. EISCAT OBSERVATIONS OF PLASMA CONVECTION AND IONOSPHERIC CURRENTS DEDUCED USING THE MAGNETOMETER CROSS

The field-perpendicular velocities observed by EISCAT at 300 km are plotted in Fig. 4. The vectors are plotted away from the circle, which is the locus of Tromsø's position in the geomagnetic latitude–local time reference frame. Local noon is at the top of the diagram. The point A at 1000 UT marks the start and end of the run. The plot to the left shows values for each 5 min post-integration, that to the right averages of the 5 min values every 20 min, giving improved clarity at some times.

4.i. *Flows in the afternoon sector*

Data from all three sites is only available from 1300 UT on 25 November. Between this time and a data gap at 1630 UT, flows are large (up to 1 km s^{-1}) and westward. At the start there is a small northward component (not obvious on the diagram) which becomes small and southward by 1630. Millstone Hill and Chatanika radars have often observed considerable northwards components at this local time for the latitude of EISCAT (Evans *et al.*, 1980; Foster *et al.*, 1982), suggesting a broad day-side entry region near noon. The behaviour in Fig. 4 is, however, similar to that observed by Foster *et al.* (1981a), which is what would be expected if the polar cap boundary were an equipotential throughout the afternoon sector and there was restricted 'throat-like' entry into the polar cap around noon. Alternatively, entry into the polar cap is shifted to the dawn side of noon (Heelis and Hanson, 1980).

The magnetograms (see Fig. 5, especially the Z-components) place the electrojet over Alta at about 1400 UT. It then broadened and swung south in an irregular manner until, by 1600 UT, it was centred near Muonio. During this time, arcs north of Muonio were seen to move southwards. All observations, then, were consistent with the normal location of the oval at this time—north of Tromsø, but decreasing in latitude with local time.

4.ii. *Effects of a Westward Travelling Surge*

Unfortunately there is a gap in the EISCAT Tromsø data between 1705 and 1725 UT, as it is in this period that a major substorm commenced (see Fig. 5). A Westward Travelling Surge (WTS), was observed by the Muonio ASC at 1709 UT and crossed the Muonio meridian at 1711 UT. All magnetometers recorded a sudden decrease in the X component and a positive spike, followed by a negative excursion, in the Y

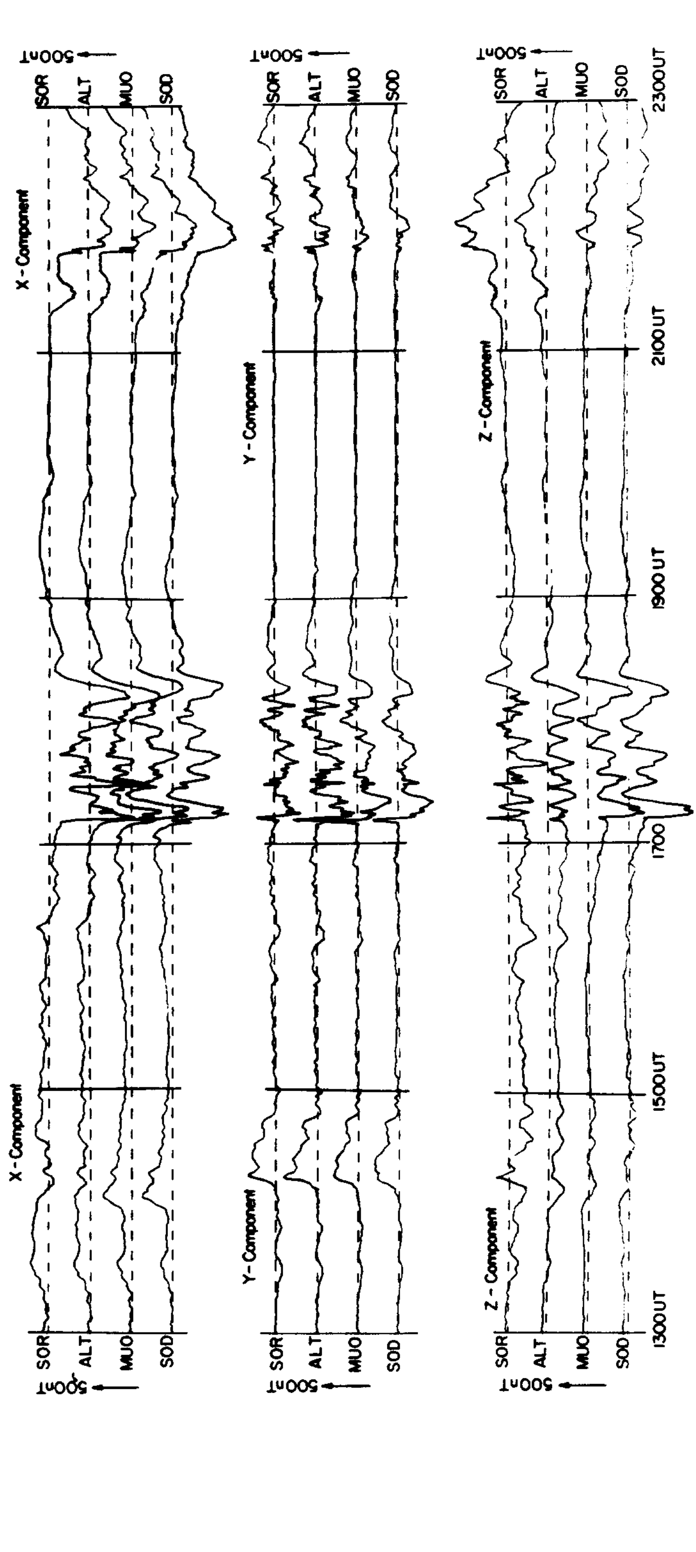

Fig. 5. Magnetograms from the magnetometer cross between 1300 and 2300 UT on 25 November 1982. See Fig. 1 for the locations of the magnetometer stations.

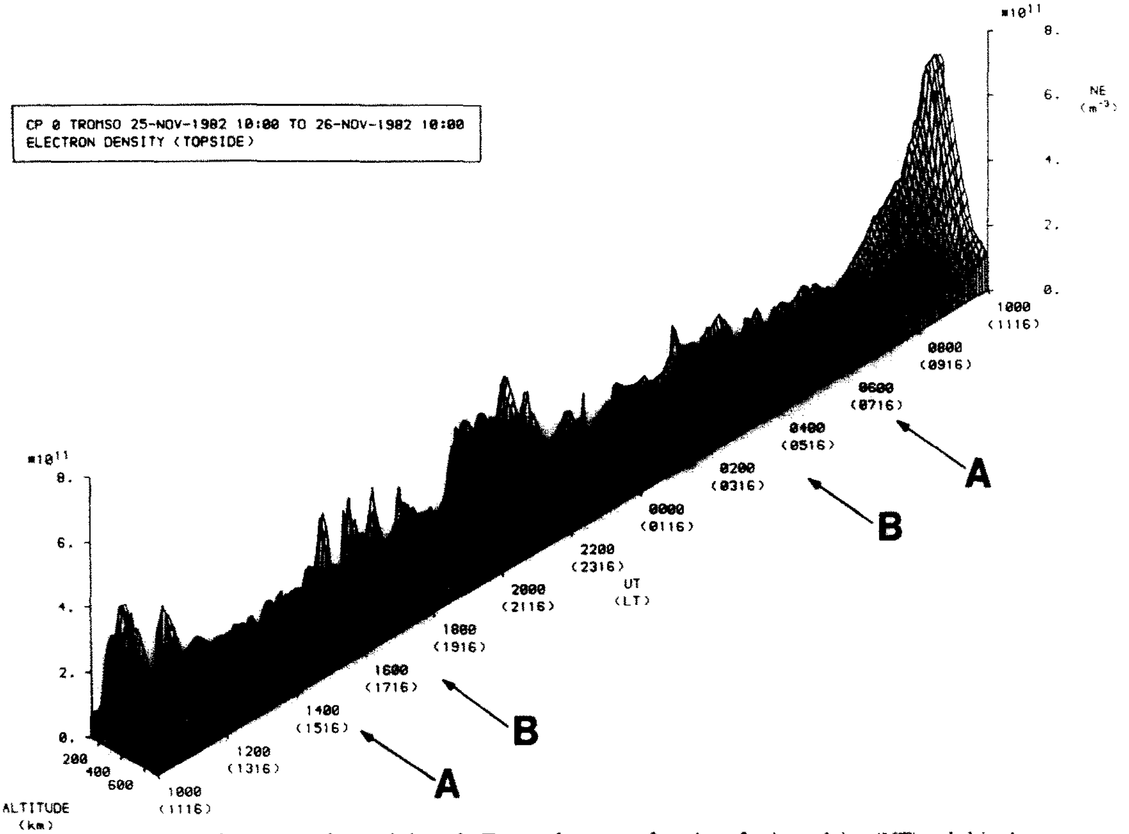

Fig. 6. Electron density, N_e, observed along the Tromsø beam, as a function of universal time (UT) and altitude, viewed from the topside. Points A mark the time boundaries for the lowest range gate in sunlight and point B similarly for the highest range gate.

component – the typical signature of a WTS (OPGENOORTH *et al.*, 1983). The spike is observed at 1710:30 at Sodankylä and 1711:30 UT at Muonio, giving a westward velocity of order 1 km s^{-1}.

The convection observed by EISCAT at the end of the data gap (1730 UT) was purely southward. A similar southward swing during a substorm in this local time sector has been described by FARMER *et al.* (1984). This is consistent with the observations of HORWITZ *et al.* (1978), who found rotation of the electric field to westward coinciding with the passage of the nose of a WTS over the Chatanika radar. This lasted about 1.5 h before northward fields returned to give westward flow. Their time resolution was only 15 min though. The EISCAT data, presented at 5 min resolution here, has been evaluated at 1 min post-integration using the remote site data and reveals a much more complex variation of electric fields immediately after the surge, consistent with that described by OPGENOORTH *et al.* (1983).

Southward turning during a substorm has also been reported by FOSTER *et al.* (1981b) for similar invariant latitude/local time. They, as here, noted the zonal flow turn eastward before returning to westward. A major difference is that they observed westward flows re-established within 1 h of the substorm, whereas in Fig. 4, the eastward component of v, the plasma flow velocity, is slightly positive until 1830–1900 UT, 80–110 min after the commencement. Note, however, that the magnetometers showed quiet electrojet re-establishment between 1820 and 1827 UT, which is also when the Muonio ASC saw a decrease in the intensity of the irregular patches and diffuse background.

4.iii. *The Harang current discontinuity and the separatrix between convection cells*

The re-established, quiet eastward electrojet south of Muonio then moved north, its centre crossing the latitudes of Muonio at 1917 UT, Alta at 1930 UT and Sørøya at 1940 UT (see Fig. 5, the Z-component), before a gradual transition to weak westward current. Negative perturbation of the X component was first seen by the magnetometer at Sodankylä at 1925 UT, by Muonio at 1948 UT and by Alta and Sørøya at

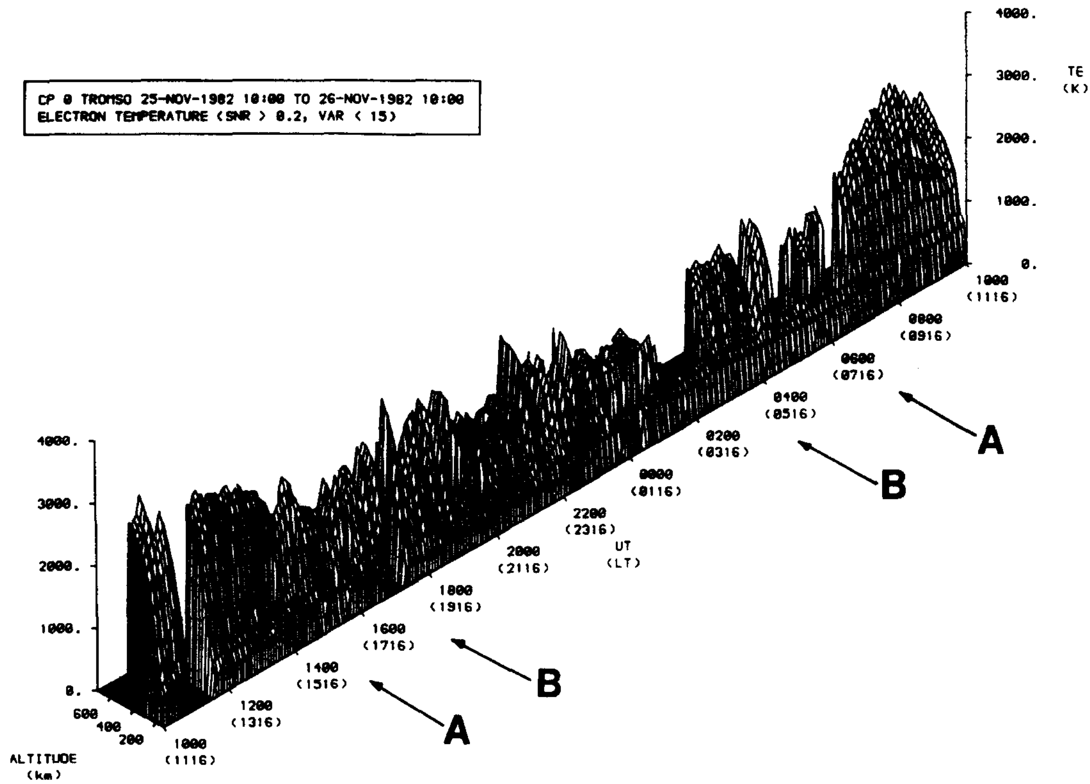

Fig. 7. Electron temperature, T_e, observed along the Tromsø beam, as a function of universal time (UT) and altitude, viewed from the bottomside. Points A and B as for Fig. 6.

1955 UT. This negative perturbation was short-lived, and another hour elapsed before westward current was firmly established. This implies a slow eastward co-rotation of the discontinuity, similar to that observed following a substorm by HORWITZ *et al.* (1978). The *F*-region flow reversal from westwards through south to eastwards was also spread over a long period of local time. ISEE-3 was, about this time (allowing for a time lag to the spacecraft), recording northwards B_z, so the convection pattern may also have been shrinking.

If one adds the complications of possible eastward co-rotation and shrinkage to the uncertainties in the shape of the dawn/dusk terminator, the data available are insufficient to separate time and space ambiguities. It is only possible to say that the Harang discontinuity is seen on the magnetograms somewhere between 1945 and 2045, while the dawn–dusk cell separatrix is seen by EISCAT at about 2120 UT. The time delay between these (65 ± 30 min) has not previously been reported.

4.iv. *Effects of northward IMF and a second substorm near local midnight*

The weak westward electrojet, established by 2045 UT, was centred slightly to the north of Muonio, and the ASC showed weak arcs to the north. That Tromsø is still south of the auroral oval suggests that the plasma convection pattern is the contracted one, with the slower convection speeds usually associated with a northwards IMF. Again this ties in with what ISEE-3 was measuring at the time. The flow rotation seen by EISCAT at 2120 UT coincided with an enhanced westward electrojet, but at 2149 UT a second substorm commenced (see Fig. 5). The Muonio ASC shows a diffuse brightening of the whole sky between the elevations of 15° north and 50° south and a new, bright arc at 20° north. The resulting enhanced conductivity produced a stronger westward electrojet, centred over Muonio, which then moved northward along with the visual aurora. The EISCAT plasma velocity observations show a slight swing to southward flow and an increase in flow speeds. Hence, in general, behaviour of the convection pattern was largely as reported for previous substorm observations, with an enhancement of flow speeds and an expansion of the pattern (HEPPNER, 1972; FOSTER *et al.*, 1981a,b).

Subsequently, the aurorae retreated northwards, and by midnight the ASC showed clear sky and EISCAT measured slow and irregular, predominantly eastward flow, with no consistent north–south component.

4.v. *Flows in the dawn sector*

In the dawn sector there was no immediate change to the previously established slow, irregular convection. Near 0600 UT, stronger north-eastward flows, consistent with two-celled convection, were re-established, but soon decayed into irregular flow shortly before the end of the tristatic EISCAT data at 0700 UT.

5. ELECTRON DENSITY PROFILES OBSERVED BY EISCAT

The electron densities observed along the Tromsø beam, N_e, are plotted in Fig. 6. Time runs up the diagram to the right. The altitude runs *down* the left-hand scale, so one views the profile from the topside. Densities have not been ionosonde-calibrated, for the same reasons as given in Farmer *et al.* (1984), but are probably accurate to 10–15%. Allowances for possible changes in receiver gain or transmitter power must be made when considering the density features shown.

5.i. *Densities in the afternoon sector*

There is a sudden decrease in densities near 1200 UT, when $NmF2$ falls by a factor of two in about 20 min. This is a real geophysical change, not a variation of the system constant or the transmitted power, since it is seen also on the Tromsø ionograms. Note, too, that the variation is different at different heights—it is hardly seen at all at the lowest heights.

The sudden change in F-region N_e in the afternoon sector is in sharp contrast to the gradual rise with time seen in the morning sector. There, from the time (0600) at which the lower atmosphere emerges into sunlight, the electron density rises. In the afternoon sector the F-region is in sunlight at all local times prior to about 1700, yet the density cut-off is at 1200. An explanation for this could be the speed of the F-region convection at that time. In the morning quadrant, flow rates are small and so on emergence into day-time the F-region has plenty of time for ionisation to build up. In the afternoon sector the flows are so fast that the F-region plasma may well have no time for the production processes to make a significant impact.

Although 3-site plasma velocities, and hence the perpendicular plasma flow directions, are not available before 1300, it is possible that the sudden density change at 1200 UT corresponds to the separatrix between dawn and dusk flow cells. 1200 UT is about 1320 local time, so if this is the day-side entry region for the polar convection, the flows in the afternoon sector would have only 2–2.5 arc-h of local time (i.e. about 2000 km) in sunlight, compared to 6 h for the morning side, a further factor in explaining the differences in ionisation densities. Since the flow pattern of Fig. 4 shows velocities of 1–2 km s^{-1} in the afternoon quadrant, the plasma there is exposed to photo-ionisation for only a few tens of minutes. A third factor is the enhanced loss rate of O^+ ions due to the increased collision frequency with N_2 induced by the high velocities (Schunk and Raitt 1980).

It is also possible that the sudden change at 1200 UT is Tromsø's entry into the mid-latitude trough. The N_e values seen here, around 10^{11} m^{-3}, are typical of the trough. As explained in the Introduction, Tromsø is expected to intersect the trough in the afternoon sector, but it is not usually expected so far round towards noon. The exit from the trough's northern wall would not necessarily be obvious if it became confused with the substorm later. Without a latitudinal scan, one cannot be certain if this is indeed the trough, but Sojka *et al.* (1983), Holt *et al.* (1983) and Evans *et al.* (1983) have observed extensions of the trough into the day-side.

Note that the discontinuity in N_e values at 1000 UT is not surprising, since the values there are 24 h apart. There is no reason to suspect, for instance, that the data from the 26th, if continued, would have a sudden fall off at the same local time as on the 25th, since flow conditions may have changed considerably.

5.ii. *Effects of the Westward Travelling Surge*

The electron density and temperature were slightly enhanced at all heights for the first available data after the surge (1715 UT, 5 min after the WTS). Meng *et al.* (1978) showed that enhanced precipitation occurred at all energies in the fronts of various surges observed by the DMSP/32 satellite. However the response of the topside ionosphere would not be observed so soon after the surge (Roble and Rees, 1977: Sojka and Schunk, 1983). An alternative cause of this enhancement is plasma produced in the quiet time auroral oval before the surge and subsequently transported southward by the equatorward convection (Fig. 4).

Following behind the surge, the Muonio ASC observed a region of non-uniform diffuse precipitation, which is a general feature of Westward Travelling Surges (Meng *et al.*, 1978). The precipitating flux usually increases at energies above about 1 keV, but reduces at lower energies. Hence, they give enhanced E-region densities, but are a smaller plasma source for the F-region than the quiet-time oval (Roble and Rees, 1977). During this period, F-region densities returned to their low, pre-surge values. The convection was southward at this time and, hence, plasma had probably been rapidly transported through the narrow poleward boundary of precipitation (where the energy spectrum is similar to that of the surge front) and then through the region of diffuse precipitation, giving enhanced densities at low altitudes, but smaller changes at *F*-region heights.

The *F*-region density increases for a short time at 1830 UT, which may be the delayed effect of the surge precipitation the hour before. There is insufficient information from the CP0 type experiment to sort out the different effects, such as plasma flow speeds through the oval, the relative contribution from soft precipitation input to the *F*-region and the diffusion upwards of harder precipitation, or the effects of phenomena like electrodynamic lowering of the *F*-region peak (see FARMER *et al.*, 1984).

5.iii. *Enhanced* F*-region densities in the pre-midnight sector*

After a slight fall-off between 1840 and 1930, the *F*-layer densities at Tromsø began to rise. $NmF2$ reached significantly higher values of $3\text{–}4 \times 10^{11}\ \mathrm{m}^{-3}$ between 2000 and 2200 UT. This rise occurred shortly after the electrojet centre had moved north across the Tromsø beam and was presumably because a region of soft auroral precipitation was now to the north of Tromsø, and the *F*-region plasma convecting southward had had time to respond. The enhanced *F*-region straddled the zonal convection reversal and Harang discontinuity, so this plasma would have recently emerged from the polar cap (HEELIS and HANSON 1980). If anti-sunward convection over the polar cap was sufficiently rapid, cleft precipitation and day-side photo-ionisation could also have contributed (KNUDSEN 1974). At the lowest heights, the arrival of a southward moving arc and subsequent diffuse precipitation caused enhancement at low altitudes from 2020 UT.

5.iv. *Effects of northward IMF and the second substorm*

The second substorm, which began at 2149 UT, moved a broad band of diffuse aurora into the Muonio ASC zenith and the Tromsø beam. Discrete arcs were observed to the north. Following the substorm, the visual auroral and the electrojet centre retreated northward to a contracted oval location, typical of a northward IMF orientation. This behaviour is similar to that of precipitating electrons observed by the ISIS satellites during substorms in prolonged periods of northward IMF (WINNINGHAM *et al.*, 1975). Enhanced *E*-region densities and riometer absorption were observed during the substorm. However, *F*-region densities decreased in a structured and irregular manner, with $NmF2$ falling from over $4 \times 10^{11}\ \mathrm{m}^{-3}$ to $1.5 \times 10^{11}\ \mathrm{m}^{-3}$. As suggested for the earlier substorm, it is possible that the plasma is being observed too soon after passage through the auroral precipitation. In addition, EVANS *et al.* (1983) have observed substorms to produce localised *F*-region depletions, considered as resulting from enhancements in the ion loss rate due to the increased electric field.

5.v. *Densities in the dawn sector*

For the observed Kp, the statistical model of HALCROW and NISBET (1977) predicts that the density should start to drop as Tromsø begins to cross the poleward trough wall, at about 0445 UT. This agrees closely with the value for numerical simulation of weak convection conditions ($\Phi = 20$ kV) by SOJKA *et al.* (1981b). The extremely low densities observed at Tromsø in the dawn sector ($NmF2 < 10^{11}\ \mathrm{m}^{-3}$) are typical of the mid-latitude trough, though they commenced near 0100 UT, much earlier than predicted by either model.

This could not be the polar hole (BRINTON *et al.*, 1978; SOJKA *et al.*, 1981a). It was further north than normally expected for the mid-latitude trough so soon after midnight, but was also probably too far south to be an example of the high-latitude trough (GREBOWSKY *et al.*, 1983). Three studies of the variations in Λ_B, the invariant latitude of the equatorward boundary of auroral precipitation, predict that it would most likely be close to, but slightly lower in latitude than, Tromsø in these conditions. However, the enhanced *E*-region densities imply that Tromsø does remain within a region of hard precipitation. No such enhancement in *F*-region densities were observed. Figure 4 shows that the eastward convection was slow during this period, hence, the plasma was largely co-rotating with the radar. Hence, if an *F*-region source had been present, there would have been sufficient time for the density to build up. This means that the characteristic energy of the precipitation must have been of the order of 10 keV, restricting the density enhancement to the *E*-region.

Once formed, the density depletion observed after 0050 UT was not filled in by auroral precipitation. Its origin, however, remains uncertain. Either the flux tubes contributing to this region had recently left the polar cap but a soft precipitation region was absent, or they had earlier passed through such a region but then spent considerable time at sub-auroral latitudes and decayed to low densities. It is possible that the substorm at 2149 UT depleted the *F*-region (EVANS *et al.*, 1983) and that the trough subsequently formed convected onto the Tromsø field line at 0100 UT. After this, the trough co-rotated with the radar and, hence, could have been a "fossil" remnant of the substorm.

The depletion is filled in by photo-ionisation as it co-rotates (with small additional eastward convection) into direct sunlight, as discussed in Section 5.i.

6. CONCLUSIONS

During the period 25–26 November 1982, strong northward electric fields persisted throughout the afternoon sector, giving eastward currents at E-region heights, as observed by magnetometers, and strong westward convection in the F-region, as observed by EISCAT. The convection was predominantly westward at the start of the observations (1500 local time), with only a small northward component. Hence, the entry region, where plasma flows into the polar cap, was either a narrow, restricted throat around noon or was shifted into the morning sector. The observed steep gradient in sub-auroral plasma density (at 1315 local time) may have been formed at the zero potential contour because the westward-convecting plasma in the dusk cell had not had time to reach such high densities as the plasma in the dawn cell, due to its far higher convection speed, a shift in the dawn–dusk separatrix to the afternoon side and possibly also the enhancement of plasma loss rates.

The passage of a Westward Travelling Surge was observed by magnetometers and an all-sky camera. The convection observed by EISCAT showed a strong swing from westward convection to southward after the surge front. The all-sky camera and magnetometer evidence showed that the polar cap boundary moved equatorward during the substorm. Following the substorm, flows returned to westward, but after a longer delay (80 min) than has been reported previously. High E-region, but low F-region, densities were observed behind the surge front.

The F-region convection rotated from westward to eastward, through southward, 65 ± 30 min after the Harang discontinuity in E-region currents was inferred from magnetometer data. F-region densities were only high when observations were made sufficiently to the south of the auroral oval for the F-layer to have responded to soft-particle precipitation.

A second substorm occurred near local midnight. As the oval is contracted, Tromsø is at a similar location, relative to the oval, as for the first substorm, despite the local time difference. For both substorms, the observations at Tromsø showed that convection was enhanced and swung southward, E-region densities were enhanced and the F-region depleted. The convection changes are consistent with an expansion of the pattern and an increase in flow speeds, without a change in the shape of the pattern. It is not clear to what extent the density changes were due to a hardening of the precipitation spectrum, increased ionospheric response times or to electric-field enhanced loss rates.

Seemingly in response to a northward IMF, the oval contracted to very high latitudes in the dawn sector. Hence, the plasma depletion observed by EISCAT is not replenished by soft auroral precipitation, although some hard precipitation produces enhancements at lower altitudes. The origin, and even the classification, of this depletion is unclear, being at a latitude between the expected locations of the high- and mid-latitude troughs, but one possibility is that it was a 'fossil remnant' of the second substorm. Convection was slow, irregular and largely eastward, hence, plasma co-rotated with the Earth round into sunlight where photo-ionisation filled the depletion.

Acknowledgements—The authors would like to thank the following members of the RAL EISCAT Section: D. M. WILLIS, A. P. VAN EYKEN, B. J. I. BROMAGE and K. S. C. FREEMAN for their support and scientific discussions. They are also most grateful to M. A. HAPGOOD, of the World Data Centre C1 for Solar-Terrestrial Physics (Rutherford Appleton Laboratory), for processing the ISEE-3 data.

The EISCAT magnetometer cross is a joint enterprise of the Finnish Meteorological Institude, Sodankylä Observatory and the University of Braunschweig. The authors are most grateful to the staff of these establishments for supplying the magnetometer and other data.

The EISCAT Scientific Association is supported by the Centre National de la Recherche Scientifique of France, Suomen Akatemia of Finland, Max-Planck Gesellschaft of West Germany, Norges Almenvitenskapelige Forsknins-gråd of Norway, Naturvetenskapliga Forskningsrådet of Sweden and the Science and Engineering Research Council of the United Kingdom. We acknowledge with thanks the assistance of the Director and staff of EISCAT.

REFERENCES

BRINTON H. C., GREBOWSKY J. H. and BRACE L. H. 1978 *J. geophys. Res.* **83**, 4767.

EVANS J. V., HOLT J. M., OLIVER W. L. and WAND R. H. 1983 *J. geophys. Res.* **88**, 7769.

EVANS J. V., HOLT J. M., OLIVER W. L. and WAND R. H. 1980 *J. geophys. Res.* **85**, 41.

FARMER A. D., LOCKWOOD M., HORNE R. B., BROMAGE B. J. I. and FREEMAN K. S. C. 1984 *J. atmos. terr. Phys.* **46**, 473.

FOSTER J. V., BANKS P. M. and DOUPNIK J. R. 1982 *J. geophys. Res.* **87**, 7513.

FOSTER J. V., DOUPNIK J. R. and STILES G. S. 1981a *J. geophys. Res.* **86**, 2143.

FOSTER J. V., DOUPNIK J. R. and STILES G. S. 1981b *J. geophys. Res.* **86**, 11357.

GREBOWSKY J. M., TAYLOR H. A. JR and LINDSAY J. M. 1983 *Planet. Space Sci.* **31**, 99.

HALCROW B. W. and NISBET J. S. 1977 *Radio Sci.* **12**, 815.
HEELIS R. A. AND HANSON W. B. 1980 *J. geophys. Res.* **85**, 1995.
HEPPNER J. P. 1972 *Planet. Space Sci.* **20**, 1475.
HOLT J. M., WAND R. H. and EVANS J. V. 1984 *J. atmos. terr. Phys.* **46**, 251.
HORWITZ J. L., DOUPNIK J. R. and BANKS P. M. 1978 *J. geophys. Res.* **83**, 1463.
HYPÖNNEN M., PELLINEN R. J., SUCKSDORFF C. and TORNIAINEN R. 1974 Technical Report 9, Finnish Meteorological Institute.
KNUDSEN W. C. 1974 *J. geophys. Res.* **79**, 1046.
MENG C.-I., SNYDER A. L. JR and KROEHL H. W. 1978 *J. geophys. Res.* **83**, 575.
MOFFETT R. J. and QUEGAN S. 1983 *J. atmos. terr. Phys.* **45**, 315.
OLIVER W. L., HOLT J. M., WAND R. H. and EVANS J. V. 1983 *J. geophys. Res.* (in press).
OPGENOORTH H. J., PELLINEN R. J., BAUMJOHANN W., NIELSEN E., MARKLUND J. and ELIASSON L. 1983 *J. geophys. Res.* **88**, 3138.
QUEGAN S., BAILEY G. J., MOFFETT R. J., HEELIS R. A., FULLER-ROWELL T. J., REES D. and SPIRO R. W. 1982 *J. atmos. terr. Phys.* **44**, 619.
REIFF P. H., SPIRO R. W. and HILL T. W. 1981 *J. geophys. Res.* **86**, 7639.
ROBLE R. G. and REES M. H. 1977 *Planet. Space Sci.* **25**, 991.
RUSSELL C. J. 1971 *Cosmic Electrodyn.* **2**, 184.
SCHUNK R. W. and RAITT W. J. 1980 *J. geophys. Res.* **85**, 1255.
SOJKA J. J., RAITT W. J. and SCHUNK R. W. 1981a *J. geophys. Res.* **86**, 609.
SOJKA J. J., RAITT W. J. and SCHUNK R. W. 1981b *J. geophys. Res.* **86**, 6968.
SOJKA J. J. and SCHUNK R. W. 1983 *J. geophys. Res.* **88**, 2112.
SOJKA J. J., SCHUNK R. W., EVANS J. V., HOLT J. M. and WAND R. H. 1983 *J. geophys. Res.* **88**, 7783
SPIRO R. W. 1978 Ph.D. Thesis, University of Texas at Dallas, Richardson, Texas, U.S.A.
SPIRO R. W., HEELIS R. A. and HANSON W. B. 1978 *J. geophys. Res.* **83**, 4255.
WHITTEKER J. H., SHEPHERD G. G., ANGER C. D., BURROWS J. R., WALLIS D. D., KLUMPAR D. M. and WALKER J. K. 1978 *J. geophys. Res.* **83**, 1503.
WINNINGHAM J. D., YASUHARA F., AKASOFU S.-I. and HEIKKILA W. J. 1975 *J. geophys. Res.* **80**, 3148.